

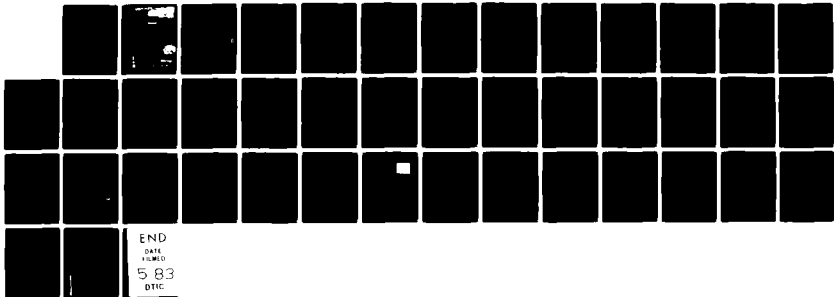
AD-A126 889

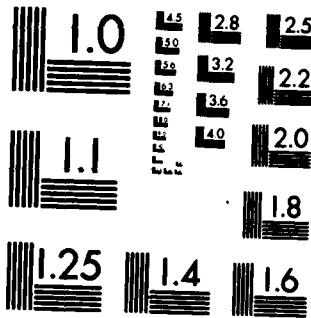
LASER PRODUCED X-RAYS FOR HIGH RESOLUTION LITHOGRAPHY
(U) BATTELLE COLUMBUS LABS OH H EPSTEIN 13 JAN 83
AFOSR-TR-83-0176 AFOSR-82-0066

1/1

UNCLASSIFIED

F/G 14/5 • NL





MICROCOPY RESOLUTION TEST CHART
NATIONAL BUREAU OF STANDARDS-1963-A

LASER PRODUCED X-RAYS FOR
HIGH RESOLUTION LITHOGRAPHY

AFOSK^{tp}-82-0066

U.S. AIR FORCE
OFFICE OF SCIENTIFIC RESEARCH

January 13, 1983

3

Interim
~~Final~~ REPORT

on

LASER PRODUCED X-RAYS FOR
HIGH RESOLUTION LITHOGRAPHY

^{to}
AFOSR-82-0066

U.S. AIR FORCE
OFFICE OF SCIENTIFIC RESEARCH

January 13, 1983

DTIC
COLLECTED
APR 15 1983
H

by
Harold Epstein

AIR FORCE OFFICE OF SCIENTIFIC RESEARCH (AFOSR)
NOTICE OF REVISIONS
This technical report is the property of the Air Force Office of Scientific Research and is loaned to your organization. It and its contents are not to be distributed outside your organization.
MATTHEW J. [unclear]
Chief, Technical Information Division

BATTELLE
Columbus Laboratories
505 King Avenue
Columbus, Ohio 43201

UNCLASSIFIED

SECURITY CLASSIFICATION OF THIS PAGE (When Data Entered)

ST 105010

| REPORT DOCUMENTATION PAGE | | READ INSTRUCTIONS BEFORE COMPLETING FORM |
|--|---|--|
| 1. REPORT NUMBER AFOSR-TR- 83-0176 | 2. GOVT ACCESSION NO. <i>AD-A126 889</i> | 3. RECIPIENT'S CATALOG NUMBER |
| 4. TITLE (and Subtitle) LASER PRODUCED X-RAYS FOR HIGH RESOLUTION LITHOGRAPHY | | 5. TYPE OF REPORT & PERIOD COVERED INTERIM 15 Dec 81 - 1 Jan 83 |
| | | 6. PERFORMING ORG. REPORT NUMBER |
| 7. AUTHOR(s) Harold Epstein | | 8. CONTRACT OR GRANT NUMBER(s) AFOSR-82-0066 |
| 9. PERFORMING ORGANIZATION NAME AND ADDRESS Battelle Columbus Laboratories Columbus, Ohio 43201 | | 10. PROGRAM ELEMENT, PROJECT, TASK AREA & WORK UNIT NUMBERS 61102F 2301/A8 |
| 11. CONTROLLING OFFICE NAME AND ADDRESS AFOSR/NP Bolling AFB, Bldg. #410 Wash DC 20332 | | 12. REPORT DATE 13 Jan 83 |
| | | 13. NUMBER OF PAGES 39 |
| 14. MONITORING AGENCY NAME & ADDRESS (if different from Controlling Office) | | 15. SECURITY CLASS. (of this report) Unclassified |
| | | 15a. DECLASSIFICATION/DOWNGRADING SCHEDULE |
| 16. DISTRIBUTION STATEMENT (of this Report) Approved for public release; distribution unlimited | | |
| 17. DISTRIBUTION STATEMENT (of the abstract entered in Block 20, if different from Report) | | |
| 18. SUPPLEMENTARY NOTES | | |
| 19. KEY WORDS (Continue on reverse side if necessary and identify by block number) | | |
| 20. ABSTRACT (Continue on reverse side if necessary and identify by block number) The laser-plasma interaction is characterized to gain an understanding of the spectrum of x-rays emitted by the plasma. The potential use of the radiated x-ray for lithography is explored. | | |

DD FORM 1 JAN 73 1473

UNCLASSIFIED

SECURITY CLASSIFICATION OF THIS PAGE (When Data Entered)

ABSTRACT

It has been demonstrated that a relatively small, high repetition rate laser can be a most attractive high average power source of x-rays in the 3/4 to 2 keV range. This x-ray energy range is particularly significant for x-ray microlithography of integrated circuits. Mode locked Nd-YAG lasers focused to several tens of μm spot sizes are very efficient x-ray sources for this purpose. Over ten percent of the laser light can be converted to x-rays of energy over 1 keV with a 400 mj 200 psec laser. Mode locked lasers with repetition rates of 10Hz and the above outputs are available now. Applicable laser systems with much higher average power should be available in the near future.

Conversion efficiency with 1.5 nsec pulses of 10 j have also been studied and preliminary results look very encouraging. However, the data analysis have not been completed, and more experimental work may be required. The high average power slab laser system under development at Stanford (1) is planned to produce 1.06 μm pulses in this range.

DTIC
COPY
INTEGRATED
2

| | |
|--------------------|-------------------------------------|
| Accession For | |
| NTIS CS&I | <input checked="" type="checkbox"/> |
| DTIC TAB | <input type="checkbox"/> |
| Unannounced | <input type="checkbox"/> |
| Justification | |
| By _____ | |
| Distribution/ | |
| Availability Codes | |
| Dist | Avail and/or Special |
| A | |

Interim REPORT

on

LASER PRODUCED X-RAYS FOR
HIGH RESOLUTION LITHOGRAPHY

to

U.S. AIR FORCE
OFFICE OF SCIENTIFIC RESEARCH

from

BATTELLE
Columbus Laboratories

January 13, 1983

INTRODUCTION

It is well established that x-ray lithography is an effective means for replicating sub-micrometer linewidth patterns⁽²⁾. Besides replicating test patterns, the technique has been used to fabricate surface acoustic wave devices, bubble domain devices, pn diodes, bipolar transistors, and MOS transistors. The basic concept of x-ray lithography is to use the short wavelength of an x-ray source instead of the long wavelength of an ultraviolet source. This essentially eliminates the diffraction limitation of the ultraviolet source. With this eliminated, x-ray lithography is capable of producing line patterns with a "line width accuracy" of less than 0.1 μm .

The laser-plasma x-ray source has developed into the most intense laboratory x-ray source available in the energy range of $\sim 3/4$ to 2 keV. In addition it appears to be the most attractive laboratory high-average-power x-ray source in this energy range, which is particularly significant for microlithography of integrated circuits. There can be little doubt about the need for high intensity and high-average-power x-ray sources which operate in this energy range, and which are small enough to be used in a laboratory or industrial locations. The rapid growth of synchrotron x-ray facilities demonstrates the increasing importance of high-average-power soft x-ray sources. However, the synchrotron is excluded as a labora-

tory x-ray source because of its size and cost. The commercial applications should expand greatly when the source becomes readily available at the home facility of the user.

The principal remaining problem in high resolution x-ray lithography is the development of an adequate soft x-ray source. The optimum x-ray energy for the few micron thick silicon masks and present photoresists is about 1.25 keV. The conventional rotating anode x-ray machines are very inefficient in this energy regime and have source diameters too large to produce high resolution at a reasonable distance. Although high conversion efficiency of laser pulses to x-rays was achieved more than 10 years ago, some of the research required to develop high-average-power sources in the most useful pulse energy ranges still remains to be done.

In this report, the development of the laser plasma x-ray source for soft x-ray lithography on integrated circuits will be discussed. This application utilizes the high-average-power of soft x-rays attainable with a rapidly pulsed laser of smaller pulse size. Other applications such as microradiography of thin samples, EXAFS (extended x-ray absorption fine structure), and medical treatment should also benefit indirectly.

BACKGROUND

This section discusses the basis of plasma x-ray sources with emphasis on the laser-plasma source⁽³⁻⁹⁾ as applied to x-ray lithography applications.

Comparison of Plasma Sources

Comparison of various plasma x-ray sources for lithography application is complex because at least three plasma parameters are involved: plasma temperature, radiating area, and conversion efficiency of energy absorbed in the target to plasma x-rays. Almost all plasma x-ray sources of interest for x-ray lithography are thin radiators in the energy range of interest. That is, the reabsorption of the x-rays by the plasma is negligible, and the dominant spectral shape of the emitted x-rays follows the plasma bremsstrahlung envelope and not that of a black body emitter. This does not mean that K, L, or M lines will be absent from the plasma. They will be present in large numbers but the statistical envelope of the radiation energy intensity will have the approximate shape $\exp(-h\nu/kT)$ where $h\nu$ is the photon energy in keV and kT is the plasma thermal energy in keV. The energy E_p incident on the photoresist is given by

$$E_p = C_1 / 2\pi r^2 \int_0^{\infty} \exp[-\alpha x - (h\nu)/kT] d(h\nu) \text{ J/cm}^2 \quad (1)$$

where $\alpha(\text{cm}^{-1})$ and $x(\text{cm})$ are the absorption coefficient and thickness respectively of the open part of the mask, r is the distance from source to photoresist and C_1 is a constant depending on the laser pulse energy, pulse width, and target. For laser pulses on copper, which are currently being considered for the high average power source, C_1 is approximately $.1E_L$. For a silicon mask below the K-edge, $\alpha = 5000(h\nu)^{-3}$. With these assumptions we find,

$$E_p = .1 E_L / (2\pi r^2) \int_0^{\infty} \exp[-5000(h\nu)^{-3} x - (h\nu)/kT] d(h\nu) \text{ J/cm}^2 \quad (2)$$

The x-rays emitted from the plasma fall off exponentially with increasing energy, while the x-ray transmissivity of the mask, $T(h\nu)$ is controlled by the photoelectric absorption cross-section and falls off rapidly with decreasing energy. The resultant x-rays reaching the photoresist fall in a narrow band as shown in Figure 8, and for the purposes of this analysis can be treated as monoenergetic with energy given by the peak $(h\nu)_m$. For silicon this is given by

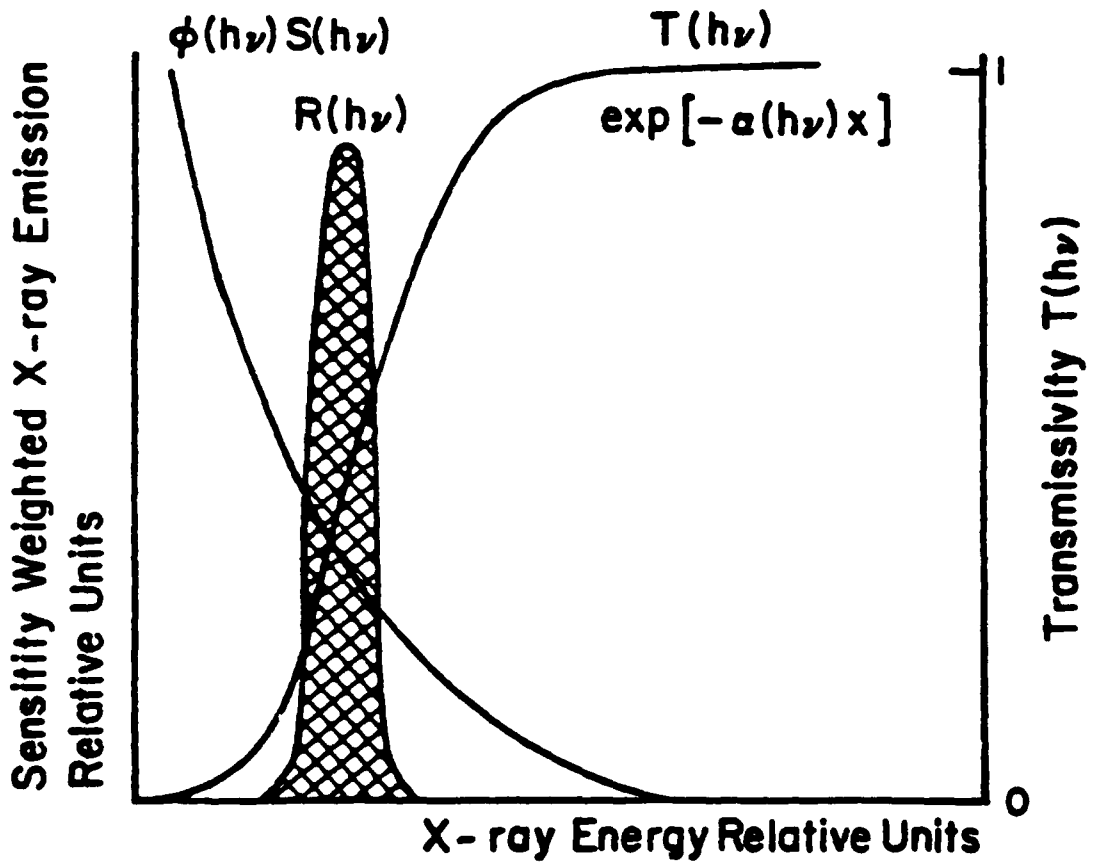


FIGURE 1. SENSITIVITY WEIGHTED X-RAYS ON PHOTORESIST

$$(h\nu)_m = 11 x^{1/4} kT^{1/4} \quad (3)$$

Because of the sharply peaked integrand, when kT is less than $(h\nu)_m$, Eq. 2 can be evaluated by expanding the integral in a Taylor series about $(h\nu)_m$ (saddle-point method), giving

$$E_p \approx .07 E_L r^{-2} (kT)^{5/8} x^{1/8} \exp(-14.7 x^{1/4} / kT)^{3/4} \text{ J/cm}^2 \quad (4)$$

For a 3 micrometer silicon mask and an 0.9 keV temperature plasma (typical of the laser-plasma), $(h\nu)_m = 1.41$ keV. The peak is sufficiently below the 1.84 keV K-edge of silicon to permit our analysis to be valid. The amount of photoresist exposure which would have resulted from x-rays above 1.84 keV is small.

Now if we consider a typical photoresist, without absorption edges in the region of $(h\nu)_m$, the absorbed dose, D , is approximately proportional to $(h\nu)^{-3}$. Thus from Eqs. 3 and 4,

$$D \propto (kT)^{-1/8} x^{-5/8} \exp(-14.7 x^{1/4} / kT)^{-3/4} \quad (5)$$

Since the coefficient of the exponent is only very weakly dependent on (kT) , the dose to the photoresist is essentially exponentially dependent on $(kT)^{-3/4}$. For a mask of 3 micrometers silicon and a (kT) of 0.9 keV, the exponential attenuation is 8.1. The silicon K-edge will cause severe attenuation if (kT) is increased by more than a factor of 2 and a (kT) of 1.8 keV still has an exponential attenuation of ~ 3.5 . Therefore the dose for the present laser-plasma source is only a little more than a factor of 2 less than that of the optimum plasma bremsstrahlung spectrum. It is nearly an optimum source for lithography.

I know of no electrical spark source producible with machines of reasonable size and cost that will produce a plasma of more than about 0.1 keV. The x-rays emitted by this type of plasma will have an exponential attenuation of over 10^4 . Many discharge plasmas emit higher energy

non-thermal x-rays. But the spectrum normally includes a hard component which causes an unacceptably weak contrast between exposed and unexposed areas.

Two other factors must also be considered in comparing plasma sources: source size, and conversion efficiency of energy absorbed in the target to x-rays. The obvious effect of source size is on resolution. At a source-to-wafer distance, D , and a mask-to-wafer distance, S , a flat disc x-ray source of radius, r , produces a "blur", δ of $\delta = S(2r/D)$. Probably of greater significance than the blur is the opportunity to bring the x-rays from a small source out of the vacuum through differentially pumped orifices and avoid the rather large x-ray attenuation through thick windows. Laser plasma sources are generally much smaller in volume than sparks.

The significance of the conversion efficiency of energy absorbed in the target to x-rays in a useful energy band is somewhat more subtle. A low conversion efficiency means that a large amount of target debris is generated with the x-rays. This debris can damage and plate windows in addition to damaging orifices for differential pumping. Even if a spark source produced sufficient x-rays for lithography, the debris would make it a difficult source to use.

Scaling Criteria

For the high-average power applications, it is advantageous to use a low pulse energy, high repetition rate laser. The high conversion rates of laser energy to x-rays (up to 27% over 300 eV) at Battelle have been achieved in the near steady-state coronal plasma radiation regime with carefully pre-conditioned plasma profiles. The rule of thumb dividing line between steady state and time dependent coronal plasmas is given by $t \approx 10^{12}/n_e$. Since the critical plasma density, where the principal absorption occurs is $n_e = 10^{21}$, radiation times greater than 1 nanosec can be reasonably assumed to be steady state. Actually a large fraction of the absorbed energy is conducted to, and radiated from, regions of greater density than 10^{21} , so somewhat shorter irradiation times can still be considered likely to be described by a steady state

radiation model. This is an important factor if we are to assume, for scaling purposes, that the radiated x-ray spectrum depends only on the power density and electron density gradient at the critical-density surface. If quasi-steady state conditions have not been achieved, the spectrum will depend on previous irradiation history.

The focal diameter, D_f , at the critical surface of the plasma changes as the plasma moves out at a velocity v . If the laser is focused on the critical density surface at time t , D_f is given by

$$D_f = f D_B \Delta + v|t|f \quad (1)$$

where f is the f number of a perfect lens, D_B is the incoming beam diameter, Δ is the natural beam divergence, and v is the plasma velocity. The first term represents the initial focal diameter on the critical surface and the second is the increase in diameter due to the expanding plasma. The situation in which the laser is focused at the position which the critical density surface will occupy when the laser reaches peak power corresponds to $t = 0$ when the laser power is at its maximum. However, for purposes of scaling, this is not a factor.

The power density at focus, P , is given by

$$P = 4/\pi [f^2 D_B^2 \Delta^2 / P_L + 2v|t|D_B \Delta / P_L + v^2 t^2 / (f^2 P_L)]^{-1} \quad (2)$$

where P_L is the laser pulse power. In the steady state v , is a function only of P for a given target. If f and Δ are kept constant and t and D_B are scaled as $P_L^{1/2}$, P will remain unaffected. Thus, the spectrum and conversion efficiency will be conserved with this scaling. This type of scaling has been tested at Battelle over a laser pulse energy range of over 100, and found to be valid.

For typical conditions of $P \approx 2 \times 10^{13}$, the copper plasma will be about 19 times ionized at the maximum plasma temperature of ~ 0.9 keV and $v \approx 3 \times 10^7$ cm/sec. The optimum f number for the lens is given by

$$f_{\text{opt}} = \left(\frac{vt}{D_B \Delta} \right)^{1/2} \quad (3)$$

Of course the f number of the lens cannot change with time on a nano-second time scale. For a high average power system we would like to have P exceed a threshold for an extended time rather than have the peak power coincide with the minimum focal diameter. This also keeps v relatively constant through a large part of the pulse. Plasma velocity is a weak function of P anyway. Choosing the lens to optimize the power at time τ gives

$$P \approx \frac{P_L}{\pi v \tau D_B \Delta} \quad (4)$$

In scaling, τ is proportional to the pulsewidth.

If high conversion efficiency is desired for low energy pulses, a short pulse width is required. However, it is not obvious why low energy pulses are desirable for a high average power laser source. Large pulse, solid state lasers are almost universally made of glass. Because of the thermal expansion and low pumping efficiency of glass, it is several times more expensive to obtain the same average power from a glass system than a YAG system. Unfortunately YAG rods are limited to small diameters (1 cm or less for commercial systems). It is, therefore, advantageous to be able to operate with low energy pulses. Since our past experience has shown that P should exceed $\sim 2 \times 10^{13}$ W/cm², a pulse energy under 1 Joule requires a pulse width less than 1 nanosec. Such a pulse width can only be attained on commercial systems by mode locking, and available mode-locked systems become unstable at pulse widths longer than ~ 0.25 nanosec. At this pulse width the ~ 1 cm diameter YAG rod is limited to 0.3-0.4 Joules per pulse if long life is required. These conditions are more than adequate to exceed the requirement that $P \gtrsim 2 \times 10^{13}$ but conversion efficiencies of laser light to x-rays of the desired energy have not been determined for pulses of this low energy in the time dependent coronal regime prior to the present study.

RESULTS OF CURRENT RESEARCH

The results of the research to date in this program have been very encouraging. It was shown in the discussion on laser energy scaling that the desired conversion efficiencies should be attainable if the following scaling condition is met.

$$E_L / v \tau^2 D_B \Delta \gtrsim 10^{14}$$

where E_L is the laser energy in joules, τ is the width of the laser pulse at half maximum, v is the plasma velocity in cm/sec, D_B is the beam diameter in cm, and Δ is the beam divergence in radians. This condition assumes an optimum lens and plasma steady state conditions, as well as optimum preparation of the plasma at the surface of the target. Since a high repetition rate mode locked laser is now available commercially with an energy of 400 mj at a pulse width of 0.2 n sec and a pulse rate of 10 Hz, these single pulse conditions were chosen for our experimental study. To go from single pulse x-ray production to a repetitive pulse system it is only necessary to devise a rapid target changing mechanism.

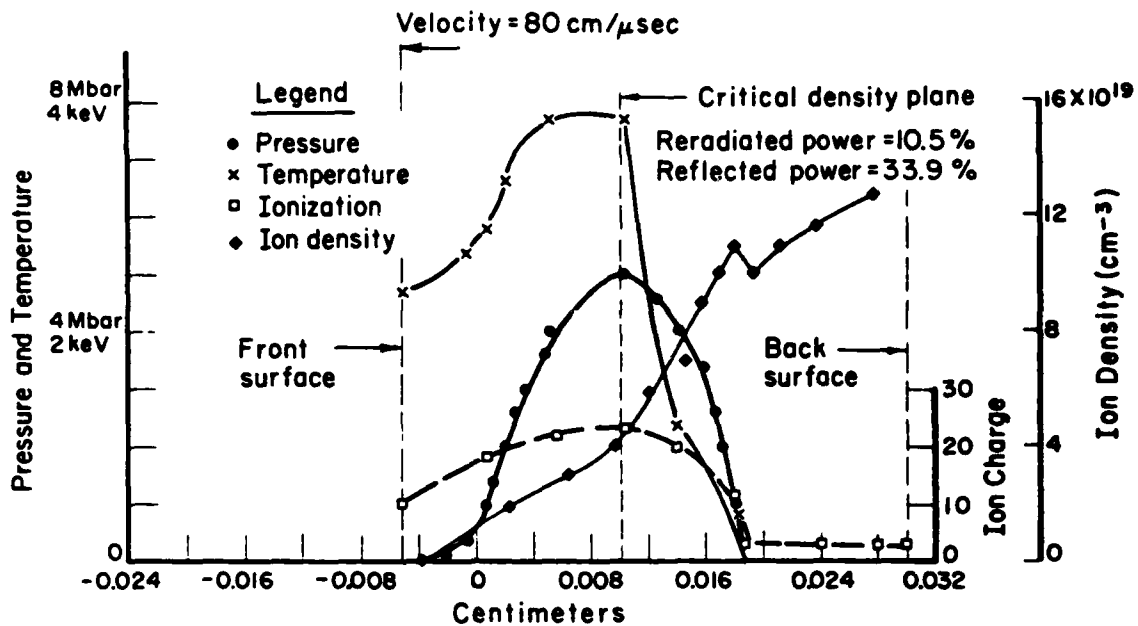
The mode locked laser pulse conditions easily meet the scaling condition equation. The major unknown factors are whether the plasma approaches steady state conditions in 0.2 n sec and whether the correct surface plasma can be realistically produced. A computer analysis done with Battelle's Flash code shows the state of ionization as a function of time for a 1-dimensional constant laser irradiation on iron assuming time dependent state ionization conditions. It can be seen from Figure 2 that the time dependent ionization has reached over 90 percent of its nanosecond value in 265 picoseconds. Since the ionization levels involved are closely spaced L levels, one would not expect to see a significant decrease in the energy of the line radiation.

The experimental results showed this conclusion to be valid in the range of interest. As shown in Table I, the conversion efficiency of laser energy to x-rays up to 2 keV is about the same for several hundred mj, 200 picosecond pulses as for 100 j, 1.5 n second pulses.

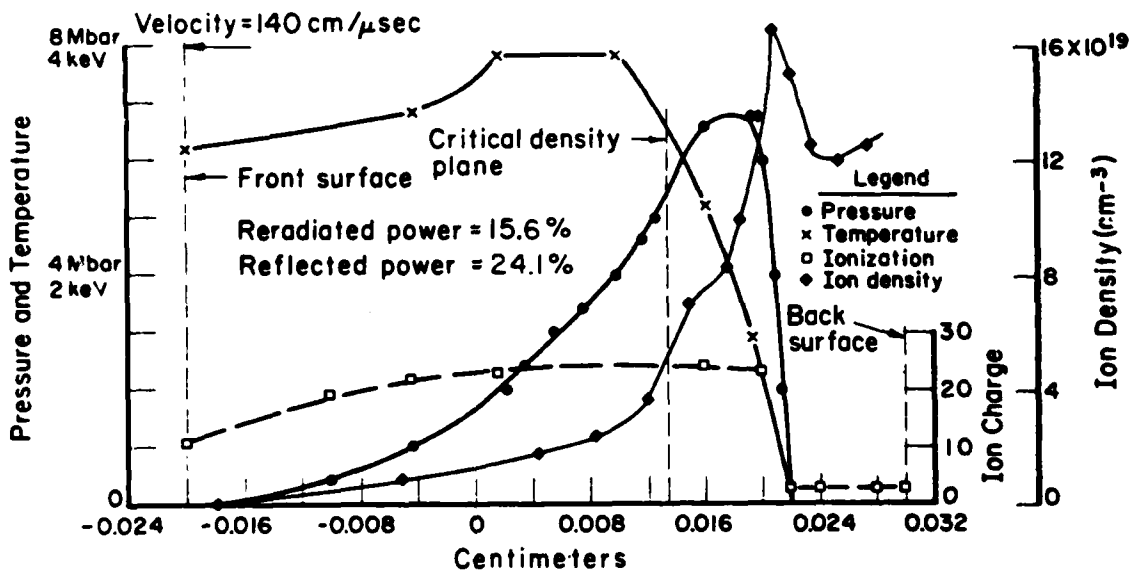
Copper targets were used for the scaling studies because copper has the atomic number corresponding to the most effective conversion efficiency, as shown in Figure 3. To understand the reason for the peak, one can consider that L-lines are caused mainly by inelastic collisions between free electrons and ground state ions. The collisions excite bound electrons from the L-shell to the M-shell, and the x-rays are produced by the spontaneous radiative decay of M-shell electrons back to the L-shell. Targets with Z above the copper peak have energy gaps between the various L and M subshells that are too wide to be efficiently excited. For targets with Z below the peak, the various energy gaps between L and M subshells increasingly fall below the 1 keV as Z decreases. In addition, the L-shell population decreases.

Targets with various combination of elements were tried but they were consistently less efficient than the most effective element in the alloy. While copper appears to be the best choice for a system which uses a Nd doped laser, the Al peak is also interesting. This peak consisted predominately of He-like K-line with an energy of 1.60 keV. This energy is interesting because it will pass readily through the K-edge notch of a Si mask substrate. While the conversion efficiency is very low (only ~1 percent), it is expected that this efficiency can be improved by irradiation with shorter wavelengths of laser light. The increased initial density should help the Al K-line radiation because the number of available radiative transition between the L and K subshells is not sufficient to radiate away the increasing power at the optimum temperature. Several high repetition rate, short wavelength excimer systems may be promising with Al targets. Experiments with frequency doubled pulses of 0.53 μm are planned in the near future.

Additional discussion of the current research is found in the two papers to be published included with this report. The abstract of a paper presented earlier this year is also included.

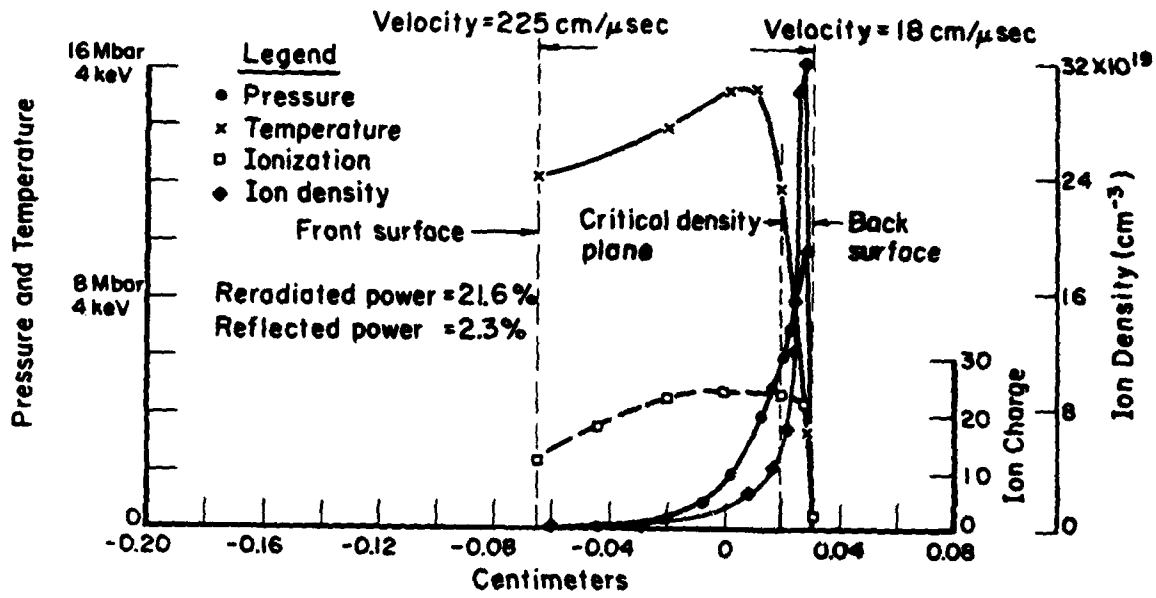


(c) Time = 135 Picoseconds

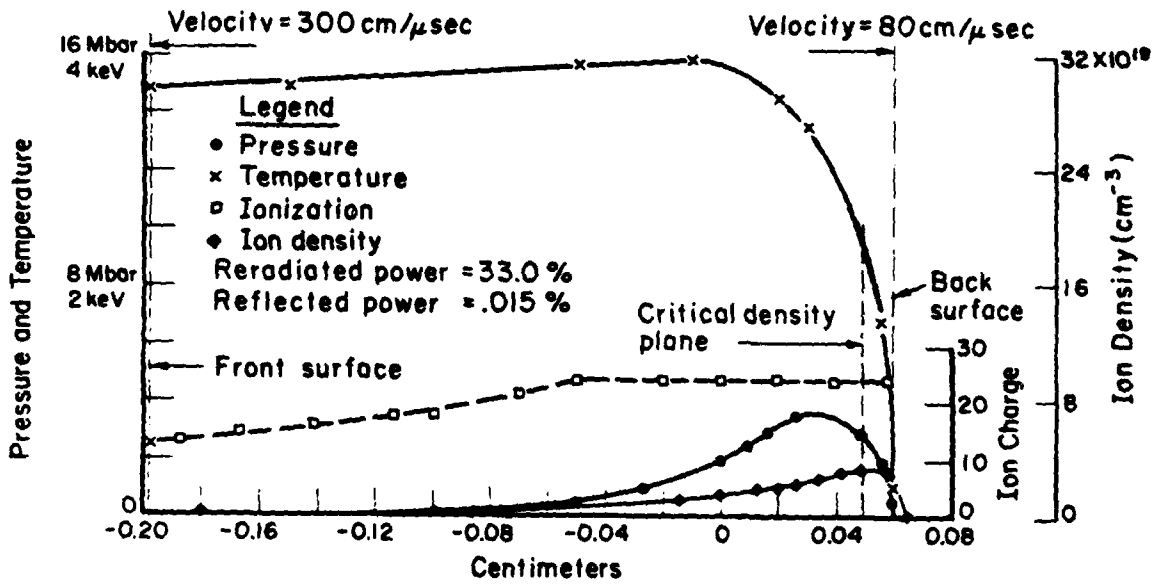


(d) Time = 265 Picoseconds

FIGURE 2. Time Dependent Coronal Model



(e) Time = 500 Picoseconds



(f) Time = 1000 Picoseconds

FIGURE 2. (CONTINUED)

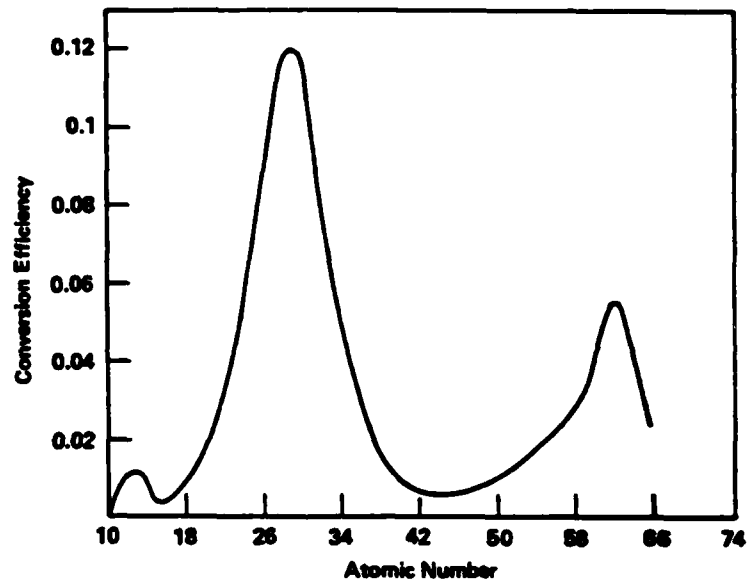


FIGURE 3. Dependence of X-Ray Conversion Efficiency Above 1 keV on Atomic Number for $1.06 \mu\text{m}$, 10^{14} W/cm^2

TABLE I. Comparison of Recent 500 mj Subnanosecond
with Previous 1.5 Nanosecond 100 j Tests

| Be-Thickness, mils | Effective Energy keV | Conversion Efficiency Above Effective Energy | |
|-----------------------|----------------------------|---|----------------|
| | | 500 mj-200 psec | 100 j-1.5 nsec |
| 5 | 1.21 | 0.12 | 0.096 |
| 1 | 1.43 | 0.050 | 0.058 |
| 2 | 1.71 | 0.032 | 0.032 |
| 3 | 1.89 | 0.020 | 0.021 |
| 5 | 2.14 | 0.008 | 0.012 |
| 10 | 2.55 | 0.004 | 0.0053 |
| 15 | 2.82 | 1×10^{-4} | 0.003 |

TABLE II. Comparison of Recent 200 mj Subnanosecond Differential Foil Spectra with Previous 1.5 Nanosecond, 100 j Tests

| Be Thickness Mils | Effective Energy keV | Conversion Efficiency Above Effective Energy | |
|----------------------|----------------------------|---|----------------|
| | | .26 j-200 psec | 100 j-1.5 nsec |
| 1/2 | 1.21 | .12 | .096 |
| 1 | 1.43 | .049 | .058 |
| 2 | 1.71 | .031 | .032 |
| 3 | 1.89 | .0065 | .021 |
| 5 | 2.14 | 7.7×10^{-4} | .012 |
| 10 | 2.55 | 2.5×10^{-4} | .0053 |
| 15 | 2.82 | 2.4×10^{-5} | .003 |

REFERENCES

- (1) Eggleston, J. M., Kane, T. J., and Oyer, R. L., "Slab Geometry Solid State Lasers" in CLEO '82, p 112, Technical Digest, Phoenix, Arizona (April, 1982).
- (2) Smith, H. I. and Flanders, D. C., Japanese J. Appl. Phys. 16, Suppl. 16-1, pp 61-65, (1977).
- (3) Mallozzi, P. J., Epstein, H. M., and Schwerzel, R. E., "Laser-Produced Plasmas as an Alternative X-Ray Source for Synchrotron Radiation Research and for Microradiography", Adv. X-Ray Anul., 22, (edit. by Gregory J. McCarthy, et al.), pp 267-279, Plenum Press (1979).
- (4) Epstein, H. M., Duke, K. M., and Wharton, G. W., "Laser-Generated X-Ray Microradiography Applied To entomology", Trans. Amer. Micros. Soc., 98 (3), pp 427-436 (1979).
- (5) Mallozzi, P. J., Schwerzel, R. E., Epstein, H. M., and Campbell, B. E., "Laser-EXAFS: Fast Extended X-Ray ABSorption Fine Structure Spectroscopy with a Single Pulse of Laser-Produced X-Rays", Science, 206, pp 353-355 (October, 1979).
- (6) Mallozzi, P. J., Schwerzel, R. E., Epstein, H. M., and Campbell, B. E., "Fast EXAFS Spectroscopy with a Laser-Produced X-Ray Pulse", Physical Review A., 23 (2), pp 824-828 (1981).
- (7) Mallozzi, P. J., Epstein, H. M., Jung, R. G., Applebaum, D. C., Fairand, B. P., Gallagher, W. J., Uecker, R. L., and Muckerheide, M. C., "Laser-Generated Plasmas as a Source of X-Rays for Medical Applications", J. Appl. Phys., 45 (4), pp 1891-1895 (April, 1972).
- (8) Mallozzi, P. J., Epstein, H. M., Jung, R. C., Applebaum, D. C., Fairand, B. P., and Gallagher, W. J., "X-Ray Emission from Laser-Generated Plasmas", in Fundamental and Applied Laser Physics: Proceedings of the Esfahan Symposium (edit. by M. S. Feld, A. Javan, and N. A. Kurnit) John Wiley & Sons, Inc. (1973).
- (9) Mallozzi, P. J., Epstein, H. M., Jung, R. G., Applebaum, D. C., Fairand, B. P., and Gallagher, W. J., "X-Ray Emission from Laser Generated Plasmas", Battelle Report to ARPA Contract DAAH01-71-C-0550 (February, 1972).
- (10) Mallozzi, P. J., Epstein, H. M., Jung, R. G., Applebaum, D. C., Fairand, B. P., Gallagher, W. J., and Campbell, B. E., "A Multi-Kilojoule Short-Pulse Glass Laser and Its Use in High-Temperature Plasma Heating", Proceedings of the Fifth Conference on Plasma Physics and Controlled Thermonuclear Fusion Research (International Atomic Energy Agency) Tokyo, Japan (November 11-15, 1974).

APPLICATIONS OF X-RAYS FROM LASER PRODUCED PLASMAS

H. M. Epstein, R. L. Schwerzel, B. E. Campbell

Battelle Columbus Laboratories
505 King Avenue
Columbus, Ohio 43201

INTRODUCTION

Progress in the development of high power lasers during the past decade has opened the door to many new areas of applications. The best known, of course, is the possibility of achieving controlled thermonuclear fusion by means of laser heated plasma. However, several applications of laser plasma x-rays have more attractive current prospects. There are many points of similarity between the x-ray and fusion problem. Both, for example, require laser heating of plasmas to the kilovolt regime. But there are significant differences. The x-ray work usually involves heating of high Z materials, while the fusible materials are low Z. Most of the x-ray applications do not require target compressions, and can use simple planar targets. Additionally, neither the plasma temperature nor the laser efficiency requirements are as severe. The main effect of these differences is that the lasers for x-ray production can be much smaller and less expensive than lasers for fusion. We have recently demonstrated that x-rays can be efficiently generated with mode locked laser pulses of several hundred mj¹. The characteristics that differentiate a laser plasma x-ray source from conventional sources are:

- (1) The x-ray spectrum comes from highly stripped species and is predominantly L line radiation or continuum in the kilovolt regime. Helium-like K lines are also obtainable.
- (2) The pulse width is very short in the ~0.1 to 10 ns range.

(3) The source size is very small, ~ 10 -200 μm diameter.

This combination of characteristics makes possible several applications which have been unattractive with conventional laboratory x-ray sources. Most applications of soft x-rays fall into two main categories; chemical analysis and x-ray microscopy. Chemical analysis includes several specialized soft x-ray spectroscopies which require x-ray sources of very high brightness. Laser-plasma x-ray sources provide peak power densities on the order of 10^{14} watts/cm² and average power densities of over 10^5 watts/cm². They are the highest peak brightness laboratory sources of x-rays in the 0.5 to 2 keV range available. The average brightness is only exceeded by synchrotrons which are not currently available in the typical laboratory. Several new x-ray spectroscopy techniques require high brightness x-ray sources; e.g., Extended X-ray Absorption Fine Structure (EXAFS), and Photon Stimulated Ion Desorption (PSID). The very high peak powers available with laser-plasma x-ray sources also permit time dependent spectral analyses of fast transient events. The low energy of the x-rays are well suited for evaluations around the K edges of the low atomic number elements. This is particularly significant for the various biological fields and for organic chemistry in general.

Applications in the x-ray microscopy category generally require a high peak or average x-ray power depending on whether transient events are involved. However, high brightness is usually of secondary importance. Examples of imaging applications are: x-ray microlithograph of integrated circuits, selective imaging, near contact microradiography, grazing incidence reflection microscopy, and x-ray fluorescence imaging. The applications require soft x-rays, which can be produced by laser plasma sources.

The plasmas most effective for the type of x-ray production of interest in this paper consist of high Z materials raised to the 1 kilovolt regime in temperature and optimized for the emission of L lines and continuum radiation. Typical conversion efficiencies of laser light to x-rays in the 1-2 keV range are over 10 percent. The absorption, ionization, hydrodynamics, and radiation process in high Z plasmas are complex. In view of this complexity, it will be valuable to discuss the basic phenomenology when an intense laser beam strikes a high Z plasma target. For the sake of definiteness, a power density of $\sim 10^{14}$ w/cm² is assumed. This also avoids most of the problems of nonlinear interactions associated with higher power densities.

MACROSCOPIC DESCRIPTION

In this section the absorption and radiation processes are characterized qualitatively.² The first consideration is to ensure

that an appreciable fraction of the laser light is absorbed in the plasma and not reflected away. When the laser frequency ω_l is less than the plasma frequency $\omega_p = (4\pi n_e e^2 / M)^{1/2}$ of the target plasma, the incident light is reflected. For the 1.06 μm radiations from Nd glass or YAG the critical electron density is $\sim 10^{21} \text{ cm}^{-3}$, so to avoid reflections laser light must be absorbed in the plasma region for which $n_e \gtrsim 10^{21} \text{ cm}^{-3}$. This description of light reflection is simplistic and not always true, but it provides a useful starting point for a qualitative description.

The second consideration is the absorption of the laser light in the underdense plasma. In order to ensure a high conversion efficiency most of the light must be absorbed in this region. Thus the conversion efficiency is dependent on the density gradient of the plasma near the critical density region. Since the beam is focused on the target and the critical density boundary moves first away from then into the target, the effective irradiation area changes with time. The useful pulse width is determined by the velocity of the critical boundary and the f number of the focusing lens.

The third consideration is the x-ray radiation from the plasma. This is predominantly line radiation and includes a large number of highly excited L lines. Continuum and plasma bremsstrahlung radiation also contribute particularly above the L line energy band. The plasma is essentially transparent to the x-rays above $\sim 1/2 \text{ keV}$. Although the absorption of laser light occurs near the critical density boundary, the high plasma thermal conductivity causes a large heat flow into the overdense plasma region and most of the radiation comes from the over-dense plasma.

MICROSCOPIC DESCRIPTION

We are now in a position to characterize the microscopic nature of the plasma. The overriding feature in this realm is that the plasma particles are not in local thermodynamic equilibrium (LTE). One nanosecond is long enough for the electrons to equilibrate among themselves by coulomb collisions and be characterized by an electron kinetic temperature, T_e . Similarly, there is enough time for the ions to equilibrate among themselves at an ion kinetic temperature, T_i . But there is generally insufficient time for T_e and T_i to become equal. What usually happens is that the incident laser light is absorbed by the electrons, which rise in temperature relatively rapidly while slowly heating the ions by electron-ion collision.

The Saha Equations³ definitely break down for the plasma of interest here, and the ion distribution is out of equilibrium.⁴ The relative ion populations are determined by the competitive balance between collisional ionization and two-body radiative recombination, in which a free electron recombines with an ion and the

excess energy and momentum are carried off by a photon. These processes are not statistical inverses of one another: the ionization process is purely collisional, whereas the recombination process involved a photon.

Although the Saha equations do not apply, the ion distribution is often still in a quasi-steady, though nonequilibrium, state. The ionization equations in this case are tractable as those for equilibrium, the main difference being that the Saha Equations are replaced by another set of quasi-steady equations, generally known as "Coronal Equilibrium" equations.

Unfortunately, in a laser heated plasma, quasi-steady conditions do not always prevail. This may be established by a rule of thumb given by McWhirter⁴; this rule states that quasi-steady conditions break down if the characteristic time for hydrodynamic expansion or contraction, τ_h , satisfies the relation $\tau_h < 10^{12}/n_e$. If this condition is satisfied, the plasma is in an extremely nonequilibrium state. To specify the instantaneous ionization state, it is necessary to know not only the local free electron conditions, but their entire past history as well! The only recourse in such a situation is to solve rate equations which include the principal microscopic processes that contribute to the ionization rate, and calculate the time development of the plasma from an initial state.

The ionization of a multikilovolt laser generated plasma requires the time dependent treatment. In the underdense plasma "skin", where $n_e < 10^{21}$, the full time dependent treatment is required, although in the overdense "core" (which can be heated by shocks and thermal conduction), a quasi-steady treatment is generally valid.

ENERGY SCALING

For the high-average power applications, it is advantageous to use a low-pulse-energy, high-repetition-rate laser. The high conversion rates of laser energy to x-rays (up to 27% over 300 eV) at Battelle have been achieved in the near steady-state coronal plasma radiation regime with carefully preconditioned plasma profiles. The critical plasma density, where the principal absorption occurs is $n_e = 10^{21}$. Using the rule of thumb for the steady state, $\tau_h > 10^{12}/n_e$ radiation times greater than 1 ns can be reasonably assumed to be steady state. Actually a large fraction of the absorbed energy is conducted to, and radiated from, regions of greater density than 10^{21} , so somewhat shorter irradiation times can still be considered likely to be described by a steady state radiation model. This is an important factor if we are to assume, for scaling purposes, that the radiated x-ray spectrum depends only

on the power density and electron density gradient at the critical-density surface. If quasi-steady state conditions have not been achieved, the spectrum will depend on previous irradiation history.

For typical conditions the copper plasma will have a critical surface velocity, $v = 3 \times 10^7$ cm/sec. The optimum f number for the lens is given by $f_{opt} = (v\tau)^{1/2} (D_B\Delta)^{-1/2}$ where τ is the pulse width, D_B is the beam diameter and Δ is the beam divergence. With the optimum lens, a general scaling criterion for laser power P_L is $P_L = 10^{14} v D_B \Delta \tau$. Recent conversion efficiency studies of laser light to x-rays of the desired energy have shown that 0.2 nsec pulses of several hundred mj are efficient x-ray producers (Figure 1). To convert efficient single pulse x-ray production to high average power, it is necessary to have a high repetition rate laser and a continuously changing target. A mode-locked YAG laser which produces 10 pulses per pulse energy of 300 mj and a pulse width of 200 ps is available from Quantel. A simple target arrangement, which provides a continuous change of surface, is a cylinder advanced on a helical drive. Since each laser pulse destroys only about 10^{-4} cm² of target area, a cylinder with 100 cm² surface area will give a million x-ray pulses. Changing cylinders would be easy because the vacuum requirements are modest.

WAVELENGTH SCALING

Wavelength scaling is much more complex than energy scaling and is quite different than the scaling conditions derived for fusion experiments. This section will be limited to a qualitative discussion of the factors influencing wavelength scaling of temperature and conversion efficiency. It is not reasonable to discuss wavelength scaling for a target of fixed atomic number because Z should be optimized for any set of wavelength and power densities. We will continue to limit the discussion to an incident laser power density of $\sim 10^{14}$ W/cm². If we look at x-ray conversion efficiency above 1 keV as a function of Z for 1.06 μ m laser light (Figure 2) we see a peak with a maximum at Cu ($Z=29$). For targets with Z below the peak the L shell is too fully ionized to be an efficient L line emitter, and for targets with Z above the peak the L lines are not

— CONVERSION EFFICIENCY OF LASER LIGHT TO X-RAYS ABOVE INDICATED ENERGY

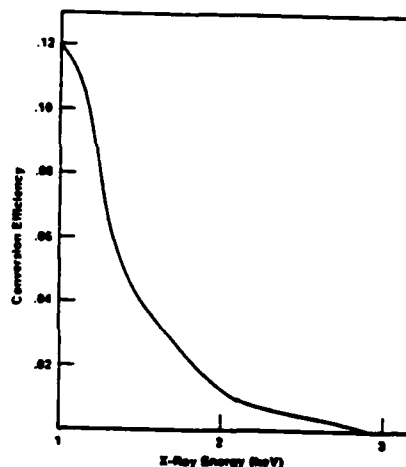


Fig. 1 Conversion Efficiency of Laser Light to X-rays above Indicated Energy

efficiently excited. The conversion efficiency for a low Z plasma can be improved by decreasing the power density as is evident from a comparison of the calculated x-ray emission for calcium ($Z = 20$) at 10^{14} and 10^{13} watts/cm² in Table 1.

The total conversion efficiency has increased from 6 to 20 percent with this factor of ten decrease in power density. However, the average energy of the emitted x-rays also has decreased substantially. A decrease in the wavelength of the incident laser light would have a similar effect. The shorter wavelength laser light is absorbed in a higher density plasma. The plasma temperature will be lower because of the higher heat capacity and radiation rate of the dense plasma. The decrease in the thermal conductivity limits the heat flow into the overdense

plasma and partially counteracts the effect of decreasing the wavelength. The degree of ionization in a coronal plasma is strongly dependent on temperature, so the over ionization of the L shell will tend to be corrected. On the other hand, if the Z of the target is higher than the peak, the opposite will be true. Increasing the wavelength will decrease the critical plasma density and increase the plasma temperature. This will usually increase the L line radiation. These qualitative arguments become more tenuous when the time dependent effects during the pulse are considered. The ionization lags the temperature so that x-ray emissions during the early part of the pulse tend to come from lower ionization states.

CONVERSION EFFICIENCY OF LASER LIGHT TO X-RAYS ABOVE 1 keV VERSUS ATOMIC NUMBER

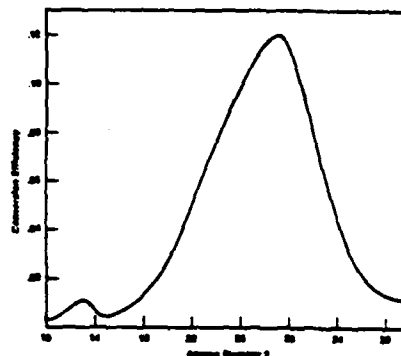


Fig. 2. Conversion Efficiency of Laser Light to X-rays above 1 keV Versus Atomic Number

For very long wavelengths the critical density is so low electron-ion collision frequencies will be small compared to the laser frequency permitting the electrons to attain high energies from the oscillating two stream instability. Very little absorbed energy will be emitted as soft x-rays. For example, CO₂ lasers with 10.6 μm wavelength are a poor choice for soft x-ray generation.

CHEMICAL STRUCTURE APPLICATIONS

In recent years, synchrotron x-ray radiation research has evolved to provide the foundations of a variety of new x-ray spectroscopy techniques for chemical analysis. Among these techniques are EXAFS, ESCA, and PSID. All of these applications require very high brightness, soft x-ray sources. Table 2 shows a comparison of the brightness of synchrotron, laser plasma x-ray, and conventional x-ray sources. The laser plasma x-ray source is slightly lower than

TABLE 2. COMPARISON OF BRIGHTNESS OF VARIOUS X-RAY SOURCES

| Source | Brightness (at keV) Photons/S-cm ² Sterad-ev |
|---|--|
| Synchrotron Doris ⁽⁵⁾ | 7×10^{20} |
| DESY | 2×10^{18} |
| Laser-plasma 10 pps- 200 ns 500 mj | 10^{17} average |
| Continuum from 60 kw ⁽⁵⁾ x-ray tube with 10^{-2} mm ² spot size | 7×10^{13} |

the DESY but far above conventional sources. Since the laser facility is much smaller and less expensive than a synchrotron, laser plasma x-rays could make the x-ray techniques that we currently employed only at synchrotron facilities accessible to a large number of laboratories which might not wish or be able to use the synchrotron⁶.

EXAFS

EXAFS is a technique for measuring the spatial arrangement of the atoms surrounding a particular atom in a molecule or crystal

lattice. It does not require the crystal structure essential to the most x-ray diffraction methods. In EXAF spectroscopy, the x-ray absorption coefficient for material is measured as a function of energy from the K or L edge of a specific element in the material to as much as a keV above the edge. Backscatter of these photoelectrons from atoms in the immediate vicinity of the absorbing atom give rise to a weak oscillation in the x-ray absorption spectrum above the edge.^{7,8,9} By analyzing their oscillation, information can be obtained about the spatial arrangement of atoms in the immediate vicinity of the absorbing species. Since long range order is not required, the EXAFS technique can be applied to the study of liquids, gases, and amorphous solids, as well as crystals.

The basic experimental configuration for EXAFS is shown in Figure 3.^{10,11} The x-ray spectrum is dispersed by Bragg reflection from a flat crystal. The crystal is chosen to have a 2d spacing slightly greater than the longest wavelength of interest and to have a low fluorescent yield for the incident x-ray spectrum. A typical crystal is RAP (rubidium acid phthalate). The x-ray spectrum can be recorded on photographic film or on a spectrographic array. The system is so arranged that the thin film sample occupies half of the x-ray beam. The dispersed x-rays thus form a double image, with the reference portion of the beam striking the top half and the sample portion striking the bottom half.

The mathematical procedures which transform the EXAFS data into information on the configuration of the atoms in a molecular or material structure are available in several articles.^{7,8,9}

ECSA and PSID

In photoelectron spectroscopy a monoenergetic photon beam excites the electrons. An intense beam of soft x-rays that can be tuned to the K or L edges of the sample is obtained from a crystal monochromator in an arrangement similar to the EXAFS. Energy analyses of the emitted electrons are done with a time-of-flight

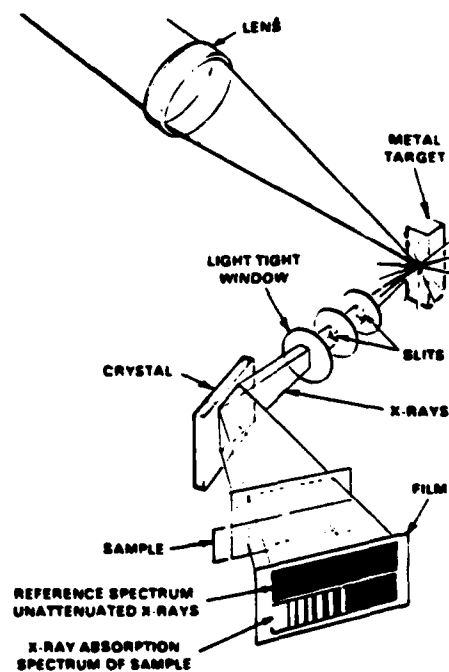


Fig. 3. Schematic View of Laser-EXAFS Experimental Configuration

spectrometer. This technique can be applied with either a single or repetitively pulsed laser-plasma x-ray source. The small repetitively pulsed source is preferable because space charge effects at the target are less severe.

In recent years ESCA has developed into a powerful technique for the investigation of the electronic energy bonds in matter. It is a particularly useful method for analyzing surface films and surface contaminants.

Electron stimulated desorption (ESD) has been a recognized method to improve the understanding of fundamental excitation and energy transfer processes mechanisms at surfaces for many years. It provides detailed information on specific species, whereas ESCA reveals only the general electron bond structure. The mechanism for ESD has been proposed to consist of a several step process. A core hole is created in a surface storm by ionizing radiation.¹³ In the subsequent Auger decay process, two or three electrons are removed from a surface anion, and the Coulomb repulsion causes desorption of a positive ion or neutral. Since the ionizing radiation is arbitrary in this model, photons can be substituted for electrons with several potential advantages. PSID can be absorbate specific, produce higher spectral resolution, and cause less perturbation by thermal effects.

The laser-plasma x-ray source is very well suited for the PSID application. A time of flight mass spectrometer can be synchronized with the repetitively pulsed system, and the high brightness and soft x-ray spectra meet the monochromator and core atom excitation requirements.

X-RAY MICROSCOPY

This section includes contact x-ray microscopy, x-ray micro-lithography of integrated circuits, and selective imaging.

Several characteristics of laser-plasma x-rays are particularly valuable for microscopy. The rapid variation of photoelectric absorption cross section with atomic number and with x-ray energy provides straightforward methods for analyzing the elements present. The x-ray wavelengths are short enough to keep resolution loss due to diffraction and electron recoil¹⁴ to a near negligible level but long enough to be absorbed with reasonable efficiency in high resolution photoresists such as PMMA. The very wide choice of line and the exponential envelope of the spectrum offer a high degree of versatility. Typical pulse widths of a few nano-second or even tens of picosecond are capable of stopping almost any motion. Peak emissions of 10 or more Gigawatts of x-rays provide single pulse exposures with sufficient photon statistics for submicron resolution.

Finally, the small source size offer high potential resolution in projection as well as near contact microradiography.

Qualitative analyses of thin samples can obviously be done most easily with a monoenergetic x-ray source. However, the exponential envelope of the plasma x-ray source also can be handled with relatively simple analyses. The energy density E_p and the x-ray image medium is given by $E_p = C/2\pi r \exp[-\alpha x - hv/kT] d hv$ (1) where $\alpha(\text{cm}^{-1})$ and $x(\text{cm})$ are the absorption coefficient and thickness, and r is the distance from source to film. For low atomic number materials which have no edges in the spectral regime of interest, α is proportional to the $(hv)^{-3}$. For example, $\alpha = 5000 \text{ hv}^{-3}$ for tissue, which is of interest in biological application.¹⁵ Quantitative analyses generally involve measuring E_p , and solving for the change in αx caused by the presence of a higher atomic number element in the specimen. This analysis is simplified by the shape of the integrand. The x-rays emitted from a laser-generated plasma fell off exponentially with increasing energy, while the x-ray transmissivity of the specimen $T(hv)$, is controlled by the photoelectronic cross section and falls off rapidly with decreasing energy. The sensitivity weighted resultant x-rays $R(hv)$ reaching the film fall in a very narrow energy band (as seen in Figure 4) and for the purposes of most radiographic analyses, can be treated as mono-energetic with the energy band dependent on the thickness and composition of the specimen. (If a normal thick emulsion x-ray film is used instead of a photoresist, the spectral sensitivity $S(hv)$ can be considered to be constant for the soft laser-plasma x-rays.) The peak of $R(hv)$ is given by $(hv)_m = 11x (kT)$. (2) Because of the sharply peaked integrand Eq 1 can be evaluated by expanding the integral in a Taylor series about $(hv)_m$ (saddlepoint method).

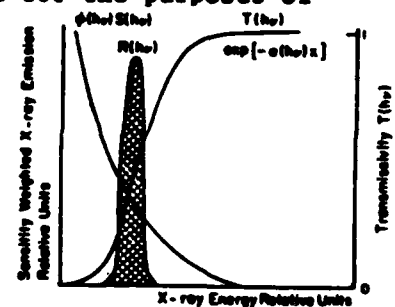


Fig. 4 Sensitivity Weighted X-Rays on Photoresist

$$E_p = C_1 r^{-2} (kT)^{5/8} \times 1/8 \exp [-14.7 \times 1/4 (kT)^{-3/4}] \text{ j/cm}^2. \quad (3)$$

X-RAY LITHOGRAPHY

It is now established that x-ray lithography is an effective means for replicating sub-micrometer line width pattern in micro-devices¹⁶. The approach is similar to contact x-ray microscopy and some of the source characterizations developed in that section will be used here. The main differences are the requirement for somewhat larger specimens between the object (mask pattern) and the recording medium (photoresist) and the necessity of precise alignment of the

mask to the photoresist for processing between multiple exposure. However, the main difference is not in the physical configuration, but in the high exposure rate required in manufacturing process.

To a first approximation the exposure time is inversely proportional to the energy absorbed per unit volume in the photoresist. If the elements in the photoresist had no edges in the wavelength regime of interest the specific absorption would be approximately proportional to γ^3 . The optimum x-ray energy will then depend on the thickness, t , and absorption coefficient of the window and mask backing. An increase in the specific dose in the photoresist for a fixed x-ray exposure can be obtained with a thinner or less absorbing mask and window, or a more absorbing photoresist. An alternative is to enhance the photoresist with an additive whose K edge is just below the incident x-ray energy¹⁷. It is also possible to minimize the mask and window absorption by choosing a material whose K edge is just above the x-ray energy.

For a laser plasma x-ray source the highest conversion efficiencies of laser light to x-rays can be obtained from excited L line radiation and the continuum just above the lines. Approximately 20 percent of the x-rays from a Cu target are transmitted through the 4 μm Si wafer used in our studies. The typical effective kT of the L line radiation is 0.85 keV, and the peak exposure comes at about 1.2 - 1.3 keV. It is also possible to excite the helium-like K lines of lower atomic number targets but the conversion efficiency of laser light to x-ray energy is almost an order of magnitude lower than for the L lines. The conversion efficiency for the helium-like K line of Al, for example, is slightly greater than 1 percent. This line has an energy of 1.6 keV and has the potential advantage that it falls in the K edge notch of Si and is attenuated very little by a few μm Si mask.

The relative merits and pitfalls of a laser-plasma x-ray device can best be seen by comparison with an x-ray lithography system based on an electron beam x-ray device. The Bell Labs system, which is probably the most advanced complete unit,¹⁷ uses the Pa L- α x-rays from a 4 kw tube¹⁸ at a wavelength of 4.4A. The mask and window are made of thin boron nitride.²⁰ The x-ray cone is expanded to the 7.5 cm wafer diameter in a helium column. The photoresist is a fast chlorinated polymer^{20,21} and 13 percent of the incident x-rays are absorbed in a 0.5 μm layer. The photoresist sensitivity is about 1.5 mj/cm^2 allowing a waver exposure to be made in 30 seconds at a distance of 50 cm from the source.

Assuming that the exposure of the photoresist is dependent only on the x-ray absorption per unit volume, the Bell photoresist will have about the same sensitivity for the 1.25 keV effective energy from the laser-plasma source as for the 2.83 keV Pa L x-rays. The Cl cross section has climbed almost back to almost the level of the

K edge peak and the cross sections of the low atomic number components are an order of magnitude higher.

The x-ray power of the Pa target x-ray machine is ~ 0.8 watt compared to ~ 0.3 watt average power for a laser plasma source based on a 10 pulse/second, 300 mj/pulse mode locked system such as the Quantel laser.²³

Window losses can be eliminated with the laser plasma x-ray system because the small source size combined with a modest pressure requirement (~ 1 torr) permit the beam to be extracted through a set of differentially pumped orifices. The beam can be expanded in a He column after the orifices. The windows of the He chamber can be very thin because there is no pressure differential.

The longer wavelength of the plasma x-ray require a thinner mask. The $3 \mu\text{m}$ Si mask absorbs about 70 percent of the exponential x-ray spectrum over 1 keV. Even if a $3 \mu\text{m}$ boron nitride window were substituted the loss would be ~ 50 percent.

If a laser-plasma x-ray lithography system were assembled from the available components, as discussed, it would be about a factor of 5 slower than the Bell system and require a thinner mask. On the other hand it would have several advantages. First, the smaller source size, less than $50 \mu\text{m}$ compared to 3mm , allows smaller ultimate resolution and potentially permits a decrease in the source to wafer distance. Second, the lower energy x-rays give better photon statistics for the same incident x-ray fluence. (The $1.5 \text{mj}/\text{cm}^2$ fluence is very near the statistical limit for $0.1 \mu\text{m}$ resolution.) Third, the contrast available with the plasma x-ray is much better. In the conventional system continuum x-rays with energies up to 25keV represent more x-ray energy than the characteristic x-rays. These can penetrate the gold easily but are not efficiently absorbed in the photoresist. Fourth, the assumed photoresist was specifically optimized for 4.4\AA x-rays. It is possible that a photoresist optimized in the same way for $1.2\text{-}1.3 \text{keV}$ x-rays might have a greater sensitivity. Fifth, it is relatively easy to put the laser system outside of the clean room and bring the laser beam in through a window, thus saving clean room space. Sixth, it is likely that much higher average power lasers will be available in the near future. This will permit a decrease in the exposure times.

A typical laser-plasma test exposure is shown in Figure 5.

SELECTIVE IMAGING

The basic technique of selective imaging is a differential x-ray absorption in which the specimen is first photographed with

an x-ray line whose wavelength is slightly greater or smaller than an x-ray absorption edge of the element to be imaged. The process is then repeated with an x-ray line on the immediate opposite side of the same edge (see Figure 6). The two photographs are then subjected to a subtraction process, and the element whose edge the two lines straddle springs into sharp relief. All other elements vanish from the picture since they absorb the two lines at essentially the same rate. The most precise subtraction is performed by digitizing the two photographs, converting film optical densities to x-ray intensity and subtracting with a computer then converting the digital image back to pictorial form. However, in its simplest conception, the subtraction can be performed optically by making a "positive" transparency of one photograph, a "negative" transparency of the other, and pressing the two together and viewing by eye. The latter technique works only with positive and negative films of carefully matched characteristics and over a limited exposure range.

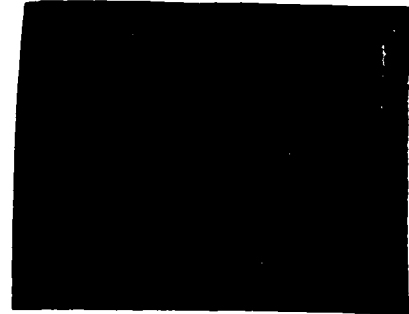


Figure 5. Typical Lithographic Pattern Made with Laser-Produced X-Rays (400X)

RELATION OF X-RAY LINES TO ABSORPTION EDGE IN SELECTIVE IMAGING TECHNIQUE DESCRIBED IN TEXT

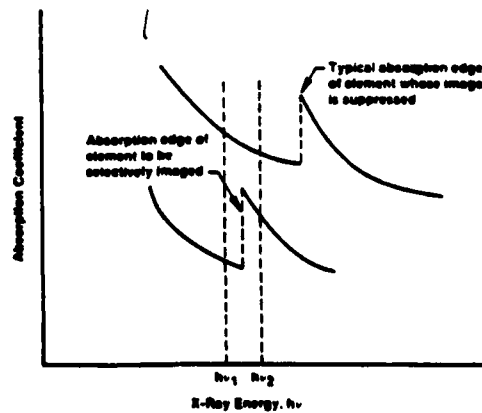


Figure 6. Relation of X-Ray Lines to Absorption Edge in Selective Imaging Technique Described in Text

The method employed in producing the initial photographs with monochromatic x-rays is contact microradiography, which was discussed in the previous sections. A large choice of x-ray lines are available for the various possible target plasmas. Intense K lines can be obtained from targets with atomic numbers up to about 20. A number of L lines can also be isolated by filtering a target with Z between 20 and 40. Weaker L lines can be selected by Bragg reflection from a curved crystal. Also energy bands of x-rays (as shown in Figure 4) can be moved above and below an edge by varying filter thickness.

CONCLUSION

The laser-plasma x-ray source provides a combination of spectrum, mask brightness, and average brightness not previously available for normal laboratory use. It promises to provide a "poor man's synchrotron" capability in a wide variety of x-ray spectroscopy and microradiography applications. Further advances in high-average power, high brightness lasers will provide major impetus to this field.

REFERENCES

1. H. M. Epstein, R. E. Schwerzel, and B. E. Campbell, "Laser Plasma X-rays for Laboratory EXAFS." CLEO '82, p. 180, Technical Digest, Phoenix, Arizona (April 1982).
2. P. L. Mallozzi, H. M. Epstein, R. G. Jung, D. C. Applebaum, B. P. Fairand, and W. J. Gallagher, X-ray Emission from Laser-Generated Plasmas, *in*: "Fundamental and Applied Laser Physics: Proceedings of the Esfahan Symposium," M. S. Feld, A. Javan, and N. A. Warnick, eds., John Wiley & Sons, Inc. (1973).
3. J. W. Bond, Jr., K. M. Watson, and J. A. Welch, Jr., "Atomic Theory of Gas Dynamics", Addison-Wesley, Inc., Reading, MA (1965).
4. R.W.P. McWhirter, Chapter 5, *in*: "Plasma Diagnostic Techniques", R. H. Huddleston and S. L. Leonard, eds., Academic Press, New York, NY (1965).
5. C. Kunz, "Synchrotron Radiation, Techniques and Applications", p. 12, Springer-Verlag, Berlin, Heidelberg, NY (1979).
6. P. J. Mallozzi, H. M. Epstein, and R. E. Schwerzel, Laser-Produced Plasmas as an Alternative X-ray Source for Synchrotron Radiation Research and for Microradiography, Adv. X-Ray Anal., 22: 267-279 (1979) (edited by G. J. McCarthy, et al.)
7. D. E. Sayers, F. W. Lytle, E. A. Stern, Adv. X-Ray Anal., 13:248 (1970);

- 15
- F. W. Lytle, D. E. Sayers, E. A. Stern, Phys. Rev.,
B11:4825 (1975);
- E. A. Stern, D. E. Sayers, F. W. Lytle, *ibid*, p. 4836.
8. S. P. Cramer and K. O. Hodgson, Prog. Inorg. Chem., 25:1
(1979).
9. C. A. Ashley and S. Doniach, Phys. Rev., B11:1279 (1975).
10. P. J. Mallozzi, R. E. Schwerzel, H. M. Epstein, and B. E. Campbell, Laser-EXAFS: Fast Extended X-ray Absorption Fine Structure Spectroscopy with a Single Pulse of Laser Produced X-rays, Science, 206:353-355 (October 1979).
11. P. J. Mallozzi, R. E. Schwerzel, H. M. Epstein, and B. E. Campbell, Fast EXAFS Spectroscopy with a Laser-Produced X-ray Pulse, Phys. Rev., A23(2):824-828 (1981).
12. H. M. Epstein, R. E. Schwerzel, P. J. Mallozzi, and B. E. Campbell, Fast EXAFS for Analysis of Transient Species, J. Am. Chem. Soc. (to be published).
13. P. J. Feibelman and M. L. Knotek, Reinterpretation of Electron-Stimulated Desorption from Chemisorption Systems, Phys. Rev., B18(12):6537-6539 (December 1978).
14. E. Spiller and R. Feder, X-ray Lithography, Chapter 3, in: "X-ray Optics", H. J. Queisser, ed., Springer-Verlag (1977).
15. H. M. Epstein, K. M. Duke, and G. W. Wharton, Laser-Generated X-ray Microradiography Applied to Entomology, Trans. Amer. Micros. Soc., 98(3):427-436 (1979).
16. H. I. Smith, D. L. Spears, and S. E. Bernacki, X-ray Lithography: A Complementary Technique to Electron Beam Lithography, J. Vac. Sci. Technol., 10:913 (Nov/Dec 1973).
17. A. Zacharias, X-ray Lithography Exposure Machines, Solid State Tech., pp 57-59 (August 1981).
18. J. R. Maldonado, M. E. Poulsen, T. E. Saunders, F. Vratny, and A. Zacharias, X-ray Lithography Source Using a Stationary Solid Pd Target, J. Vac. Sci. Technol., 16:1942 (Nov/Dec 1979).
19. D. Maydan, G. A. Coquin, H. J. Levinstein, A. K. Sinha, and D. K. Wang, Boron Nitride Mask Structure for X-ray Lithography, J. Vac. Sci. Technol., 16:1959 (Nov/Dec 1979).
20. G. N. Taylor and T. M. Wolf, Plasma-Developed X-ray Resists, J. Electrochem. Sci., 127:2665 (Dec 1980).
21. P. Duncumb, X-ray Microscopy and Microradiography, Academic Press, New York, NY (1957).
22. H. M. Epstein and B. E. Campbell, "Microlithography of Integrated Circuits with Laser Plasma X-ray Sources", CLEO '82, p. 182, Technical Digest, Phoenix, Arizona (April 1982)

ACKNOWLEDGMENTS

This work was sponsored in part by the U.S. Air Force Office of Scientific Research under Grant Numbers AFOSR 82-0066 and 78-3575. The United States Government is authorized to reproduce and distribute reprints for Governmental purposes notwithstanding any copyright notation hereon. This manuscript is submitted for publication with the understanding that the United States Government is authorized to reproduce and distribute reprints for governmental purposes.

We thank P. J. Mallozzi for his many helpful suggestions and discussions.

Laser Plasma X-Ray Source Optimization for Lithography

Harold M. Epstein, Philip J. Mallozzi and Bernard E. Campbell

Battelle's Columbus Laboratories
505 King Avenue, Columbus, Ohio 43201

Abstract

The laser-plasma X-ray source has been evaluated for submicrometer X-ray lithography exposure machines. X-ray lithography systems based on commercially available lasers of reasonable cost appear to be feasible. Such machines would make full wafer exposures of silicon slices with a throughput consistent with current manufacturing requirements.

Introduction

X-ray lithography is an extension of the near contact optical printing technique to the soft (0.25 to 3.0 keV) X-ray regime. The technology has advanced to the point where 1 micrometer linewidth patterns can be produced with a throughput of 40 to 60 wafer levels per hour, exposing 75 mm wafers. An X-ray exposure machine that will accomplish this was developed at Bell Laboratories, and uses a 4 kilowatt conventional electron beam X-ray with a stationary anode.¹

Although electron beam X-ray sources promise to be satisfactory for the first generation of machines, future development will depend heavily on the exploitation of non-conventional X-ray sources such as pulsed plasmas and synchrotrons. This is because the commercial production of linewidth patterns significantly smaller than 1 micrometer requires combinations of softer X-rays, smaller source diameter, and higher time-average X-ray power and brightness that are difficult to achieve with electron beam X-ray sources.

This paper discusses the results of an optimization study performed to determine the design parameters of a laser plasma X-ray source for submicrometer X-ray lithography. It appears that X-ray lithography exposure machines based on commercially available lasers of reasonable cost are feasible. Such machines could make full wafer exposures of 75 mm standard silicon slices with a throughput in excess of 60 wafer/levels per hour. With a moderate amount of development, a much higher throughput could be achieved. With a laser plasma X-ray source, problems plaguing submicrometer X-ray lithography such as too large a source diameter and penumbra width, too low a source power or brightness, too hard an X-ray spectrum, as well as difficulties in bringing X-rays out of the vacuum chamber into air, can all be eliminated or substantially reduced.

Basic experimental conditions

The basic experimental configuration used in generating X-rays for the lithography application is shown in the simplified sketch given in Figure 1. Typically, 1.06 micrometer wavelength neodymium laser pulses with energies ranging from .2 to 150 joules and pulsewidths ranging from 0.2 to 5 nanoseconds are focused onto a copper target to spot sizes ranging from 40 to 150 micrometers. Approximately 25 percent of the incident laser light is converted into X-rays in the 0.3 to several keV regime. Approximately 10 of the 25 percent lies between 1 and 2 keV.

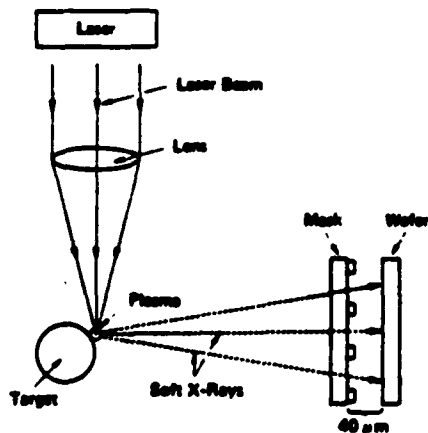


Fig. 1. Basic experimental configuration

The target is a relatively large cylinder that advances on a helical drive to present a fresh, nearly flat, surface area to successive laser pulses. Since each laser destroys only about 10^{-4} cm² of target area, a cylinder with 100 cm² of surface area will give about a million X-ray pulses.

A mask/wafer assembly is placed 10 to 50 cm from the source. The X-ray outputs which are cited refer to X-rays radiated into the 2 steradians facing the mask/wafer assembly.

Laser/target interaction and X-ray spectrum

The physical mechanism that converts the laser light into X-rays is of interest. Briefly, a specially tailored leading edge of the focused laser pulse vaporizes and ionizes the surface of the target and creates a low temperature plasma. The plasma that is created absorbs the remainder of the laser pulse by the inverse bremsstrahlung absorption process and is heated to a temperature of approximately 1 keV (1.2×10^7 °K). X-rays are produced in this high temperature plasma by bremsstrahlung, recombination radiation, and line radiation, all of which originate from electron-ion collisions.

More specifically, the X-ray outputs cited in the previous section were obtained with neodymium laser light incident on a copper target at an intensity of approximately 10^{14} watts/cm². The X-ray spectrum generated with a copper target has a large number of intense spectral lines in a spectral band centered at approximately 1.2 keV (Figure 2). These lines are emitted from a plasma layer of electron temperature $T_e \sim 1$ keV and electron density $n_e \sim 10^{21}$ cm⁻³ located near the leading edge of a thermal diffusion front that advances through the low temperature plasma during the lifetime of the laser pulse. The spectral lines are L-lines emitted from highly ionized species of copper.

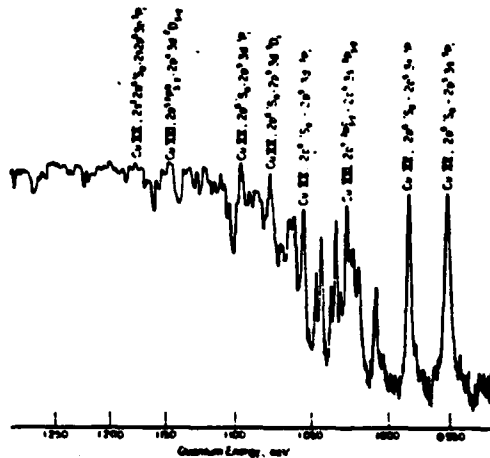


Figure 2. Densitometer tracing of bent crystal spectrograph of X-ray produced from copper target with neodymium laser pulse.

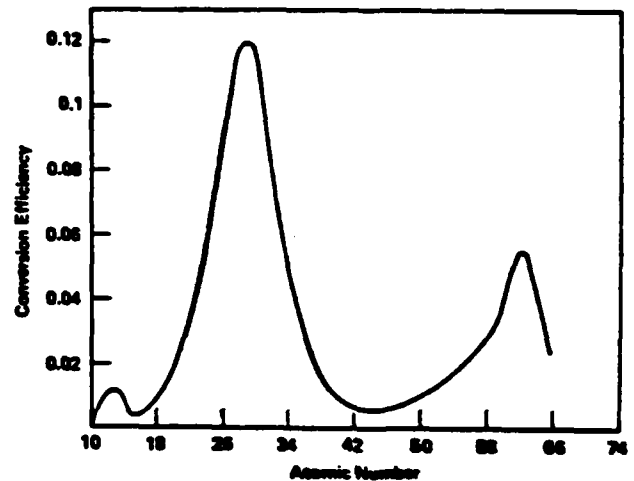


Figure 3. Dependence of X-ray conversion efficiency above 1 keV on atomic number for $1.06 \mu\text{m}$, 10^{14} W/cm².

Copper is a good choice of target. Indeed, Figure 3, which plots conversion efficiency versus atomic number Z , shows copper ($Z = 29$) to be the optimum element for converting neodymium laser light into X-rays above $h\nu = 1$ keV, assuming an incident intensity of 10^{14} watts/cm².

To understand the reason for the peak, it is helpful to realize that the L-lines are mostly caused by inelastic collisions between free electrons and ground state ions. The collisions excite bound electrons from the L-shell to the M-shell, and the X-rays are produced by the spontaneous radiative decay of M-shell electrons back to the L-shell. Targets with Z above the copper peak have energy gaps between the various L and M subshells that are too wide to be efficiently excited. Targets with Z below the peak have the problem that the various energy gaps between L and M subshells increasingly fall below 1 keV as Z decreases. In addition, the L-shell population decreases.

Laser Parameters

As noted earlier, the $1.06 \mu\text{m}$ wavelength of neodymium lasers can be converted into X-ray between 1 and 2 keV with an efficiency of ~ 10 percent. In addition, a great variety of neodymium-glass and neodymium-YAG lasers capable of doing this are available in the attractive \$25,000 to \$150,000 range. With this motivation, we will give first consideration to the $1.06 \mu\text{m}$ wavelength, at least to the point of seeing where it leads.

At a wavelength of $1.06 \mu\text{m}$ the preferred incident target intensity is $\sim 10^{14}$ watts/cm². Intensities much less than 10^{14} do not give good conversion efficiencies above 1 keV. Intensities much greater than 10^{14} lead to complications worth avoiding.

We now consider laser power P_L , laser pulse energy E , and laser pulsewidth τ . Calculations and experiments have established that the following relation must be satisfied to

obtain the good conversion efficiencies:

$$\tau_h \propto \text{constant} \times E^{1/3} \quad (1)$$

where the constant depends on target material and lens focal ratio. This formula has been verified for a large number of laser pulses ranging from .02 joules in .2 nanoseconds to 150 joules in 5 nanoseconds, incident on copper at 10^{14} watts/cm². The intuitive reasonableness of the formula can be appreciated by realizing that the focal spot diameter d to which a laser pulse must be focused to achieve an intensity of 10^{14} watts/cm² is proportional to $P_L^{1/2}$, and that for experiments using the same target material and lens focal length, the plasma will expand to an unacceptable extent with respect to the incoming cone of laser light in a characteristic hydrodynamic expansion time $\tau_h \propto d \propto P_L^{1/2}$, or $\tau_h = \text{const} \times E_{\text{max}}^{1/3}$. The last formula is equivalent to Equation (1).

One might wonder at this point why it is possible for the same conversion efficiency and spectrum to span a range of pulsewidths lying on both sides of $\tau = 10^{-9}$ seconds? The conceptual difficulty is that the plasma radiates most of the X-rays at an electron density $n_e \sim 10^{21}$ cm⁻³, so that the characteristic time required for the radiating ions to strip down to a quasisteady degree of ionization is approximately $10^{12}/n_e \sim 10^{-9}$ seconds.² The explanation is that only a thin layer of matter in the overall plasma is radiating the interesting X-rays at any given time during the laser pulse, and the time it spends radiating is a very small fraction of a nanosecond long--smaller than any of the laser pulsewidths which have been considered. The phenomenological description of the layers that successively radiate the X-rays is the same for pulsewidths down to about .1 nanosecond.

We are now in a position to select a candidate laser. What is needed is a combination of pulse energy and repetition rate that gives high time-average-power (pulse energy times repetition rate) at reasonable cost. The choice is basically between two types of high-average-power lasers that satisfy (1). One type is a subnanosecond, mode-locked, neodymium-YAG laser that delivers pulses smaller than one joule at a high repetition rate. The other is a multnanosecond, multijoule, neodymium-glass laser with a much lower repetition rate. Neodymium-YAG has the advantage of delivering a given time-average-power several times more inexpensively than neodymium-glass. Neodymium-glass, on the other hand, can give a much higher time-average-power if needed.

It is not clear at the present time what type of laser will ultimately prove most suitable. For the purposes of this paper we select YAG to see what can be done at relatively low cost. YAG rods are limited to a diameter of approximately 1 cm or less for commercial systems, which implies an energy limit of about 1/2 joule per pulse if long rod life is required.

A YAG laser is available from Quantel that delivers 0.3 joule, 0.2 ns pulses at a rate of 10 pps, or an average laser power of 3 watts. At the 10 percent conversion efficiency cited above, such a laser would yield 0.3 watts of X-ray power. In the next section we will see what might be achieved with such a source.

Geometrical Configuration and Exposure Time

The laser plasma X-ray source offers many advantages in exposure geometry and exposure time.

The small source diameter allows the mask/wafer assembly to be located much closer to the source than the 50 cm distance frequently employed with electron beam X-ray machines. It also solves the troublesome problem of designing an X-ray window to bring the soft X-rays into a helium expansion chamber. Figure 4 shows a laser plasma X-ray source located 15 cm from the mask/wafer assembly, with the X-rays directed out of the vacuum chamber through differentially pumped orifices. The first hole has a diameter of ~1 mm and is located less than 2 mm from the source, so that all of the X-rays directed at the mask will pass through the hole.

The small source diameter eliminates the penumbra problem. The penumbra width δ at the surface of the wafer is given by $\delta = \frac{d}{L} \times L$, where δ is the mask-to-wafer distance, L is the source-to-mask distance, and d is the source diameter. For definiteness, let us assume a mask-to-wafer distance of $l = 40$ μ m. Since $d \sim 40$ μ m for the 0.3 watt X-ray source, and $L = 15$ cm, $\delta \sim .01$ μ m. Linewidth unsharpness due to penumbra is therefore not a problem for linewidths down to 0.1 μ m.

Another advantage of the laser X-ray source is that the soft X-ray spectrum permits a thin layer of absorber to be used on the mask substrate, while still maintaining good contrast ratio. This reduces the aspect ratio of the absorber pattern on the mask and

decreases the expertise required in mask fabrication. The thinner absorber layer also permits a smaller source-to-wafer distance before the unsharpness due to X-rays striking the finite-thickness absorber pattern at a slant angle becomes a problem. For absorber thicknesses ranging between 0.1 and 0.5 μm , the unsharpness at the edge of the wafer due to this effect ranges from 0.2 to 0.1 μm in the geometry shown in Figure 4, which is acceptable.

The exposure times that can be achieved with a laser plasma X-ray source are highly attractive. At a distance of 15 cm, the X-ray fluence delivered to the surface of the mask in 60 seconds by the 0.3 watt X-ray source is $60 \times 0.3/2\pi \times 15^2 = .0127$ joules/cm², or approximately 13 millijoules/cm². Approximately 30 percent of this energy (about 4 millijoules) will be transmitted through a 3 μm thick silicon mask substrate and strike the photoresist coated wafer. This is more than adequate to expose a number of high-sensitivity resists currently under development. Indeed, resists with a sensitivity of 1.5 millijoules/cm² have been reported.³ Such a sensitivity would yield an exposure time of 20 to 25 seconds in the present application.

It should be mentioned that at a distance of 15 cm, the X-ray intensity varies by about 6 percent from the center to the edge of the wafer. This is partly because the edge is more distant from the source, and partly because the X-rays striking the edge have a longer path length through the mask substrate. It is possible that the 6 percent non-uniformity is acceptable. If not, the nonuniformity can be corrected by introducing an X-ray pellicle that varies in absorption from center to edge.

Future Development

The future development of laser plasma X-ray sources for lithography depends on the degree that the spacing between mask and wafer can be controlled. A variation of w micrometers in spacing will introduce an error of $w \tan \theta \sim 1/4$, and the spacing needs to be controlled to better than 1/2 micrometer.

If the spacing between mask and wafer can be properly controlled, the source-to-mask distance can be less than the 15 cm discussed earlier. In this case, a 0.3 watt laser plasma X-ray source would give good exposure times even with high resolution resists of relatively low sensitivity.

On the other hand, if the spacing between mask and wafer cannot be well controlled, the source-to-mask distance would have to be greater than 15 cm. In that case, 1 to 2 watts of X-ray power would be desirable. This could be achieved, with some development, with a neodymium-YAG or neodymium-glass laser with a time-average laser power of 10 to 20 watts. It might also be achieved with one or another of a large variety of advanced lasers with wavelengths within a factor of two or so of the neodymium wavelength.

In any event, the laser plasma X-ray source should be considered as a strong contender for submicromete X-ray lithography.

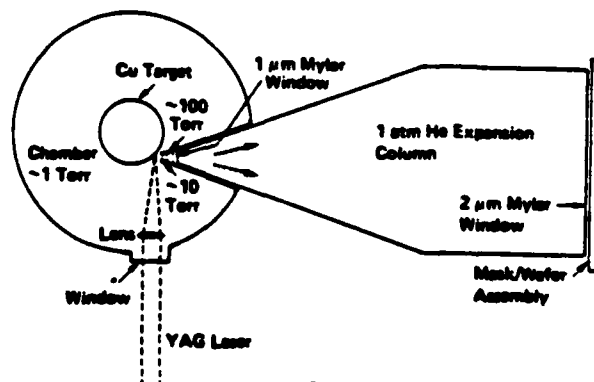


Figure 4. Experimental configuration with differentially pumped orifices.

Acknowledgements

This work was sponsored in part by the U.S. Air Force Office of Scientific Research under Grant Number AFOSR 82-0066

Bibliography

1. A. Zacharias, "X-Ray Lithography Exposure Machines," *Solid State Tech.*, p. 57, August 1981.
2. R.W.P. McWhirter, Chapter 5, in "Plasma Diagnostic Techniques," R. H. Huddlestone and S. L. Leonard, eds., Academic Press, New York, N.Y. (1968).
3. J. M. Moran and G. H. Taylor, "Improved Resolution for DCOPA Negative X-Ray Resist by Exposure Under a Controlled Atmosphere of Nitrogen and Oxygen," *J. Vac. Sci. Technol.*, V. 16, p. 2020, November/December 1979.
4. H. M. Epstein, R. L. Schwerzel, and B. E. Campbell, "Applications of X-Rays From Laser Produced Plasmas" in *Sixth International Workshop on Laser Interaction and Related Plasma Phenomena*, eds. G. H. Miley and H. H. Hora, Plenum, to be published.
5. G. A. Garrettson and A. P. Neukermans, "X-Ray Lithography," *Hewlett-Packard Journal*, V. 33, No. 8, p. 14, August 1982.
6. D. J. Nagel, R. E. Pechacek, J. R. Creig, and R. R. Whitlock, "Pulsed X-Ray Lithography," *SPIE Proceedings*, V. 135, p. 135, April 1978.
7. H. I. Smith, D. L. Spears, and S. E. Bernacki, "X-Ray Lithography: A Complementary Technique to Electron Beam Lithography," *J. Vac. Sci. Tech.*, V. 10, p. 713, November/December 1973.
8. T. E. Saunders, "Wafer Flatness Utilizing the Pin Recess Chuck," *Solid State Tech.*, V. 25, No. 5, p. 73, May 1982.
9. J. R. Maldonado, M. E. Paulsen, T. E. Saunders, F. Vratny, and A. Zacharias, "X-Ray Lithography Source Using a Stationary Solid Pd Target," *J. Vac. Sci. Tech.*, V. 16, p. 1942, November/December 1979.
10. P. J. Mallozzi, H. M. Epstein, R. G. Jung, D. C. Applebaum, B. P. Fairand, and W. J. Gallagher, "X-Ray Emission From Laser Generated Plasmas," in "Fundamental and Applied Laser Physics," M. S. Feld, A. Javan, and K. A. Warwick, eds., Wiley and Sons, New York, p. 165, 1973.

the EXAFS technique, the x-ray absorption coefficient of a material is measured as a function of energy above a K or L edge. The fine structure in this spectrum yields information on the distances of neighboring atoms. A very intense, high-brightness x-ray source is required for practical EXAFS. The energy range corresponding to K or L edges of atoms with atomic numbers up to 40 is $\frac{1}{2}$ to 3 keV. This energy range is well suited to laser-plasma x-ray sources.^{1,2}

Well resolved EXAFS spectra of A and Mg have been obtained with single pulses from a 100-J Nd:glass laser with a pulse width of 1.5 nsec focused to a spot size of 150 μm . The experimental configuration is shown in Fig. 1. Transient structure studies during phase changes have been made with this technique.

It has more recently been shown that a mode locked Nd-Yag system with a pulse energy as little as 200 mJ and a pulse width of 200 psec is a very effective x-ray source for EXAFS studies of low atomic number elements. Over 10% of the laser light can be converted to x rays of energy above 1 keV. Mode-locked systems of this energy and pulse operating at repetition rates of 10 Hz are available and offer excellent high-average power and brightness x-ray sources. (12 min)

1. P. J. Malozzi, R. E. Schwerzel, H. M. Epstein, and B. E. Campbell, *Science* 206, 353 (1979).
2. P. J. Malozzi, R. E. Schwerzel, H. M. Epstein, and B. E. Campbell, *Phys. Rev. A*, 23, 824 (1981).

FW3 Microlithography of integrated circuits with laser-plasma x-ray sources

H. M. EPSTEIN and B. E. CAMPBELL, Battelle-Columbus Laboratories, Columbus, Ohio 43201.

Very high intensity laser-plasma x-ray sources have been developed over the past ten years. In addition, it has been demonstrated that a relatively small, high repetition rate laser is a most attractive high average power source of x-rays in the $\frac{1}{2}$ to 2 keV range for general industrial or laboratory applications. This energy range is particularly significant for x-ray microlithography of integrated circuits. A relatively low-cost system with an anticipated output of a few tenths of a watt of x-rays in the above energy range will be discussed. An interesting advantage of the laser plasma x-ray source is the small source diameter, about 50 μm . This small source size will allow the x rays to be extracted from the vacuum chamber into a helium drift tube through a series of differentially pumped orifices, greatly reducing window losses. Furthermore, if the mask/water distortion problems can be solved, submicron lithography is possible with efficient large-solid-angle geometry exposures. The exponential decrease of laser-plasma x rays with increasing energy also provides good contrast between the open and masked regions.^{1,2} The hard x-ray component is a severe problem with most plasma sources created by electrical discharges or E-beams. There is little doubt that the laser-plasma x-ray source should be considered as a major contender for submicron lithography.

Mode locked Nd-YAG lasers focused to several tens of μm spot sizes are effective x-ray sources for this purpose. Over 10% of the laser light can be converted to x rays of energy over 1 keV with a 200-mJ 200-psec laser. Mode-locked lasers with repetition rates of 10 Hz and the above outputs are available now. Applicable laser systems with much higher average power should be available in the near future. (12 min)

1. P. J. Malozzi, H. M. Epstein, and R. E. Schwerzel, *Adv. X-Ray Anal.* 22, 267 (1978).
2. H. M. Epstein, K. M. Duke, and G. W. Wharton, *Trans. Amer. Micros. Soc.*, 98, 427 (1978).

FW4 Highly efficient performance of CO₂ lasers by multipass amplification

M. INOUE, H. FUJITA, D. DAIDO, K. TERAI, K. IMAMURA, M. MATOBA, S. NAKAI, and C. YAMANA-KA, Osaka University, Institute of Laser Engineering, Yamada, Suita 565, Japan.

In present CO₂ laser systems for fusion research, single-pulse amplification systems are adopted, and the maximum efficiency of these systems is a few percent.^{1,2} Higher efficiencies $\geq 10\%$, which are required for reactor drivers, could be achieved by adopting a system of multipass amplification in a single-gain media of large volume.

Following energy extraction by a short pulse, the population inversion of the laser transition is depleted, but gain recovery occurs due to fast relaxation between vibrational levels of CO₂ and N₂ molecules. In general, the energy stored in the vibrational levels of CO₂ and N₂ is not completely extracted by a single short (~ 1 -nsec) pulse. A significant fraction of this stored energy can be extracted by successive optical pulses with an optimum time interval equivalent to the vibrational relaxation time.

The gain recovery for various gas mixtures was measured by amplifying two pulses with a variable time interval, as shown in Fig. 1. In this Letko CO₂ laser experiment, the first pulse was used for the depletion of population inversion, while the second pulse was used for measurement of the gain recovery. It was seen that gain recovery of $>70\%$ was obtained after a time interval of 100 nsec independently of gas mixture. The characteristic time of relaxation and its dependence on gas mixture suggest that the relaxation of the lower laser level population to the ground level is not important and that the relaxation to the first bending level (010) is dominant in the gain recovery process.

The optimization of the gas mixture to obtain high efficiency for multipass amplification was investigated. Part of the optical pulse amplified by the gain media was reflected by the NaCl splitter and was injected into the gain media again to achieve multipass amplification. Experimental results are summarized in Table I. An efficiency of 8% was achieved by the multipass amplification, whereas the single-pass efficiency was 2%. Theoretical analysis of the present experiments shows the possibility of attaining efficiencies $>10\%$ by optimizing the multipass optical system. (12 min)

1. R. L. Carlson *et al.*, *IEEE J. Quantum Electron.* QE-17, 1662 (1981).
2. C. Yamana *et al.*, *IEEE J. Quantum Electron.* QE-17, 1678 (1981).

FW5 High-power amplification of subnanosecond CO₂ laser pulses

STEPHEN J. CZUCHLEWSKI and VICTOR O. ROMERO, University of California, Los Alamos National Laboratory, Los Alamos, N.M. 87545.

The propagation of nanosecond CO₂ laser pulses in high-power high-gain amplifiers has been well understood for several years.¹⁻⁴ However, the amplification of subnanosecond pulses has not been thoroughly investigated. In a previous experiment⁵ on the propagation of 570-psec pulses in a low-gain TEA laser, a significant discrepancy between experiment and theory was observed. It was found that the 570-psec pulses broadened to 880 psec upon amplification, whereas theory predicted that they should have narrowed to 370 psec.

For a number of experiments it is desirable to have high-power subnanosecond (FWHM ≤ 500 psec) CO₂ laser pulses. Therefore, we have studied the propagation of such pulses in a high-pressure high-gain e-beam-controlled amplifier, using one

beam of the Los Alamos Gemini laser system. The Gemini power amplifier is a triple-pass device with an output aperture of 34-cm diam and is operated at a pressure of 1900 Torr. The amplifier has a small-signal gain g_0 of 0.022 cm^{-1} and a three-pass gain-length product g_0L of ~ 13 .

To generate short pulses for injection into the amplifier, 100-mJ 1-nsec pulses were focused with $f/1$ optics into ~ 20 Torr of pure nitrogen. By varying the N₂ pressure, pulses with widths from 200 to 700 psec could be obtained. Temporal pulse shapes were monitored with fast pyroelectric detectors directly coupled to 5-GHz oscilloscopes. The response time of the detector-oscilloscope combination is ~ 120 psec.

For 5-mJ 850-psec input pulses, 0.3-TW 350-J output pulses with widths of 900 psec were obtained. With shorter 1-mJ 400-psec inputs, outputs of comparable power (0.3 TW) but shorter widths (400 psec) and reduced energy could still be obtained. Much shorter output pulses (285 psec) of reduced power and energy were also observed. These results are in qualitative agreement with the predictions of a fully coherent theoretical model,^{1,2} and a more detailed analysis is in progress. If these results scale as the model predicts, still higher peak powers and narrower pulse widths should be obtainable on the Helios laser system with its 3-pass gain-length product $g_0L \sim 20$.

In contrast to previous experiments, it appears that the present data are consistent with predictions of a coherent pulse-propagation model. This suggests that currently available CO₂ laser amplifiers are capable of producing very high peak power pulses if they are driven with fast-rising input pulses. Suitable pulses could be obtained, for example, by passing 1-nsec pulses through saturable absorbers, such as p-doped germanium. (12 min)

1. B. J. Feldman, *IEEE J. Quantum Electron.* QE-9, 1079 (1973).
2. B. J. Feldman, *Opt. Commun.* 14, 13 (1975).
3. H. C. Volk, *J. Appl. Phys.* 50, 1179 (1979).
4. E. E. Stark *et al.*, *Appl. Phys. Lett.* 23, 322 (1973).
5. S. J. Czuchlewski *et al.*, in *Proceedings, 1978 International Conference on Lasers*, V. Corcoran, Ed. (STS Press, 1979), pp. 498-505.

FW6 Quantitative laser-induced gas breakdown thresholds

CHARLES L. WOODS, Harvard University, Physics Department, Cambridge, Mass. 02138.

Recent advances in laser design provide the smooth reproducible single-mode pulses required¹ for the quantitative comparison of theory and experiment in the laser-induced breakdown of gases. This paper applies microwave breakdown diffusion theory² to our focused CO₂ laser measurements and calculates an effective diffusion length L_e and an effective pulse width T_e from the measured shape of the laser pulse. Previous laser breakdown measurements³ have used fitting parameters for values of the diffusion length and usually for the laser pulse width. The ionization rates using our calculated values of these parameters for our laser pulse are in good agreement with dc ionization rates using accepted values of the electron-neutral collision frequency for momentum exchange ν_{en} .

A single-mode 200-kW hybrid CO₂ laser⁴ was used with a carefully chosen lens to measure reproducible breakdown thresholds and avalanche growth times in clean, flowing, preionized gas samples (He, H, deuterium, Ar, and N) at atmospheric pressures.

We show that the threshold for breakdown at the peak of a smooth pulse can be closely approximated by the following equation for the ionization rate at the peak of the pulse ν_i :

DATA
FILM

5-8